

# Electrical and thermal properties of semiconducting $\text{Fe}_2\text{O}_3\text{--Bi}_2\text{O}_3\text{--Na}_2\text{B}_4\text{O}_7$ glasses

A. Al-Hajry, A.A. Soliman\*, M.M. El-Desoky<sup>1</sup>

*Physics Department, College of Science, King Khalid University, P.O. Box 9004, Abha, Saudi Arabia*

Received 28 January 2004; received in revised form 9 September 2004; accepted 13 September 2004

Available online 27 October 2004

## Abstract

$x\text{Fe}_2\text{O}_3\text{--}(25-x)\text{Bi}_2\text{O}_3\text{--}75\text{Na}_2\text{B}_4\text{O}_7$  glasses with  $x = 5, 10, 15$  and  $20$  mol% were prepared by press-quenching from glass melts, and their dc conductivity ( $\sigma$ ) were determined in the temperature range  $300\text{--}473$  K. It is found that the dc conductivity increased from  $10^{-9}$  to  $10^{-5}$   $\text{S cm}^{-1}$  with increasing  $\text{Fe}_2\text{O}_3$  content. The small polaron hopping (SPH) model of Mott is used for the interpretation of the temperature dependence of the activation energy. Results of thermal analysis performed at different heating rates on these glasses are reported and discussed. From the heating rate dependence of the glass transition temperature ( $T_g$ ) and the peak temperature of crystallization ( $T_p$ ) values of the activation energy for glass transition ( $E_t$ ) and the activation energy for crystallization ( $E_c$ ) are evaluated, and their composition dependence is discussed. © 2004 Elsevier B.V. All rights reserved.

*Keywords:* Conductivity; Crystallization; Ferromagnetism

## 1. Introduction

Extensive studies have been carried out on semiconducting oxide glasses containing transition metal ions owing to interests in their conduction mechanism and glass structure [1,2]. There are relatively few reports on  $\text{Fe}_2\text{O}_3$  containing semiconductor glasses [3,4]. Besides, some  $\text{Fe}_2\text{O}_3$  containing glasses exhibit ferromagnetic behavior [5,6]. Among Fe ion containing oxide glasses are types that exhibit magnetism; ferromagnetism is observed in glasses of  $\text{Li}_2\text{O}_3\text{--Bi}_2\text{O}_3\text{--Fe}_2\text{O}_3$  system prepared by twin roller quenching [6]. Thus, Fe ion containing glasses are likely to exhibit ferromagnetism as well as semiconduction, if any glass having a high electrical conductivity at room temperature can be obtained. Hence, the glasses are expected to be used, for example, as sensors using magnetoresistance effect. On

borate glasses, a lot of work has been going on during the last decades, especially concerning an optimization of glass preparation, investigation of properties and effects to acquire information about the structure of glasses [7,8]. Particularly the last point leads to the question of a relation or even similarity of the internal structure of chemically identical borate melts, glasses and crystals and a mutual influence on structure formation [9].

Electrical conduction of glasses containing transition metal oxides (TMOs) is known to be semi-conducting. The conduction in these glasses has been interpreted by small polaron hopping (SPH) model [10–13]. Small polarons are charge carriers trapped by self-induced lattice distortions that extend over the near surrounding [14,15]. The transport of these quasi-particles consists of phonon-assisted hopping.

When a glass material is heated at a constant heating rate in a differential scanning calorimetry (DSC) experiment, the material undergoes structural changes and eventually crystallises. In addition to the exothermal crystallization signal, the DSC trace shows an endothermic signal before crystallization signal occurs: the glass transition peak. This

\* Corresponding author. Permanent address: Physics Department, Faculty of Science, Ain Shams University, Abbassia, 11566 Cairo, Egypt.

*E-mail address:* [Alaa\\_Soliman2000@hotmail.com](mailto:Alaa_Soliman2000@hotmail.com) (A.A. Soliman).

<sup>1</sup> Permanent address: Physics Department, Faculty of Education, Suez Canal University, El-Arish, Egypt.

calorimetric glass transition is generally considered to be due to changes in the amorphous structure, which approaches a thermodynamic equilibrium state as the temperature of the system is increased [16–18]. Like the crystallization peak, the position of the glass transition signal depends on the heating rate [19]. It is, therefore, tempting to make a Kissinger plot [20] of the glass transition signal and calculate activation energy from the slope. However, whilst this procedure has been shown to yield a physically meaningful activation energy for the crystallization peak [21,22], there is no a priori reason to believe that this is also the case for the glass transition signal.

In this paper, the electrical and crystallization parameters of  $x\text{Fe}_2\text{O}_3-(25-x)\text{Bi}_2\text{O}_3-75\text{Na}_2\text{B}_4\text{O}_7$  glasses with  $x=5, 10, 15$  and 20 mol% are examined by dc conductivity and the DSC thermograms. Also, the structure of these glasses was studied before and after heat treatment using X-ray diffractometer.

## 2. Experimental

Reagent grade  $\text{Fe}_2\text{O}_3$  (99.9%),  $\text{Bi}_2\text{O}_3$  (99.9%) and  $\text{Na}_2\text{B}_4\text{O}_7$  (99.99%) were used as raw materials. The homogeneous mixture was taken in a platinum crucible and placed in a furnace. Melting was carried out in controlled conditions at temperature ranging from 1420 to  $1470 \pm 5$  K for 1 h with occasional stirring and was then poured onto a polished copper kept at room temperature and was immediately pressed by a similar copper block. The amorphous nature of the glasses and the identification of the phases crystallizing in the glass during the differential scanning calorimetry (DSC) runs were ascertained by X-ray diffraction (XRD) using a Shimadzu XRD 6000 diffractometer. Powder of each glass sample was scanned in the range from  $2\theta = 10-80^\circ$  using  $\text{Cu K}\alpha$  radiation ( $\lambda = 1.5406 \text{ \AA}$ ). The dc conductivity ( $\sigma$ ) of the as-quenched glasses was measured at temperatures between 300 and 473 K and under a constant dc voltage. The value of the current at different temperatures was measured using a picoameter (Keithley 485 Autoranging Picoameter). Silver paste electrodes deposited on both faces of the polished samples. The  $I-V$  characteristic between electrodes was verified. The thermal behavior was investigated using a Shimadzu DSC-50 differential scanning calorimeter. The temperature and energy calibrations of the instrument were performed using the well known melting temperatures and melting enthalpies of high purity tin, lead and indium supplied with the instrument. Samples in the form of powders weighing around 20 mg were sealed in platinum pans in an atmosphere of dry nitrogen at a flow of 30 ml/min and scanned from room temperature to above the exothermic peak at different heating rates ranging from 10 to 35 K/min. The values of the glass transition temperature,  $T_g$  and the peak temperature of crystallization  $T_p$  were determined using the software supplied with the apparatus.

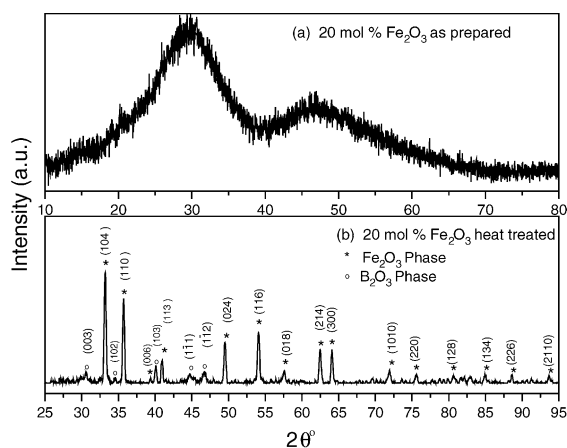


Fig. 1. XRD pattern of  $20\text{Fe}_2\text{O}_3-5\text{Bi}_2\text{O}_3-75\text{Na}_2\text{B}_4\text{O}_7$  glass: (a) as-prepared and (b) fully crystallized.

## 3. Results and discussion

### 3.1. X-ray diffraction

The XRD examination confirmed the amorphous nature of the as-prepared  $20\text{Fe}_2\text{O}_3-5\text{Bi}_2\text{O}_3-75\text{Na}_2\text{B}_4\text{O}_7$  glass as shown in Fig. 1. The powders annealed at 970 K for 2 h, showed the existence of two crystalline phases. The first and dominant phase is the rhombohedral  $\text{Fe}_2\text{O}_3$  with  $a = 5.0356 \text{ \AA}$  and  $c = 13.7489 \text{ \AA}$  (PDF2 file no. 33-0664). The second weak phase is the hexagonal  $\text{Bi}_2\text{O}_3$  with  $a = 4.3358 \text{ \AA}$  and  $c = 8.3397 \text{ \AA}$  (PDF2 file no. 72-0626). These results agree well with the behavior of as-prepared and heat-treated samples seen later from DCS curves.

### 3.2. dc conductivity

In many cases, the electrical conduction in glasses containing TMOs, have been proved to be electronic in nature. The conduction process is believed to occur by electron hopping between the ions existing in different valence states in the glass. For example, if a glass contains iron oxide, hopping will take place between the  $\text{Fe}^{2+}$  and  $\text{Fe}^{3+}$  ions



among the different factors, which influence the conductivity in the glass are the following:

1. The average distance separating ion sites (total oxide concentration).
2.  $\text{Fe}^{2+}/\text{Fe}^{3+}$  ratio (number of carriers).
3. The annealing effects on the degree of ordering (charge mobility).

Fig. 2 shows the Arrhenius plot of  $\log(\sigma)$  between 300 and 473 K. Deviation from a linear curve occurs around  $\theta_D/2$  ( $\theta_D$ : the Debye temperature). These glasses had  $\sigma$  from  $2.5 \times 10^{-9}$  to  $2.52 \times 10^{-5} \text{ S cm}^{-1}$  at temperatures from 300 to 473 K.

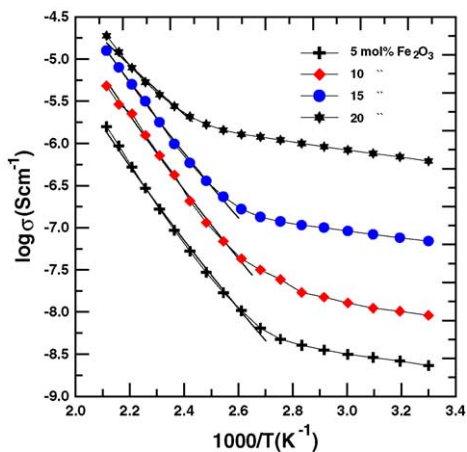


Fig. 2. Temperature dependence of dc conductivity,  $\sigma$ , for different glass compositions. The solid lines are calculated by using the least-square technique.

Fig. 2 clearly gives the linear relationship between  $\log(\sigma)$  and  $1/T$ . The slope of the curves, which gives the activation energy for conduction, however, has two different values, and increases towards higher temperatures. According to Austin and Mott [11], the electrical conductivity and temperature for the glass containing TMO is related by arrhenius equation:

$$\sigma = \left(\frac{\sigma_0}{T}\right) \exp\left(\frac{-W}{kT}\right) \quad (1)$$

where  $\sigma_0$  is a pre-exponential factor,  $W$  the activation energy and  $k$  the Boltzman constant.

In Fig. 2, the dc conductivity varied linearly against  $1/T$  at the two temperature regions, indicating that the conduction of the present system is mainly electronic [13,23]. In the low temperature region ( $T < \theta_D/2$ ), the transport is attributed to be electronic, while at the high temperature region ( $T > \theta_D/2$ ) the  $\text{Bi}^{3+}$  and  $\text{Na}^+$  ions may become mobile and participate in the conduction process, similar to that for some alkali phosphate and borate glasses containing iron [13,24].

Fig. 3 shows the plot of activation energy,  $W$ , and electrical conductivity at fixed temperature (443 K) as a function of  $\text{Fe}_2\text{O}_3$  content. It is observed that as the percentage  $\text{Fe}_2\text{O}_3$  increases the activation of electrical conduction decreases and electrical conductivity increases. Such a behavior is a feature of SPH in this system [10–13]. The high value of activation energy and low value of electrical conductivity are similar to those for  $\text{V}_2\text{O}_5\text{--BaO--B}_2\text{O}_3$  and  $\text{Fe}_2\text{O}_3\text{--Na}_2\text{P}_2\text{O}_6$  glasses [1,25].

Fig. 4 shows that the values of electrical conductivity increase as the concentration of ions increases. This is due to: (a) the small ionic size of the iron when compared with that of bismuth ion and (b) the large concentration of  $\text{Fe}^{2+}$  ions. Generally, it is known that addition of bismuth oxide to the glass decreases the electrical conductivity as a result of increase of bridging oxygen ions. This may decrease the open structure (i.e. the non-bridging oxygen ions), through which the charge carriers can move with lower mobility. This result

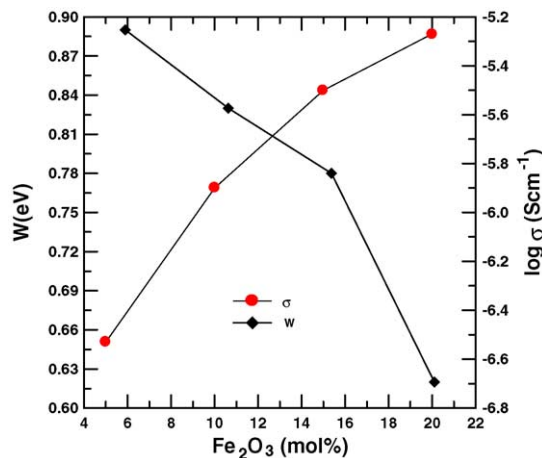


Fig. 3. Effect of  $\text{Fe}_2\text{O}_3$  content on dc conductivity,  $\sigma$ , and activation energy,  $W$ , for different glass compositions. Lines are drawn as guides for the eye.

provides the reason why the coulombic binding force of the bismuth ion is affected by the type of transition metal ions (TMI), which is located at a neighboring site. The change in the binding force may cause the change in the bismuth ion mobility (bismuth ion is probably not very mobile), due to the large difference in ionic sizes of Fe and Bi leading to the smaller values of mobility and increase of stability and decrease of conductivity [26,27]. On the other hand, increasing of non-bridging oxygen ions with increasing iron oxide may increase the thermal stability of the present glasses (see Fig. 6)

### 3.3. Thermal analysis by DSC

Typical DSC curves of the as-prepared  $20\text{Fe}_2\text{O}_3\text{--}5\text{Bi}_2\text{O}_3\text{--}75\text{Na}_2\text{B}_4\text{O}_7$  glass as recorded at different heating rates are shown in Fig. 5. The characteristic features of the investigated thermal curves were as follows; firstly an

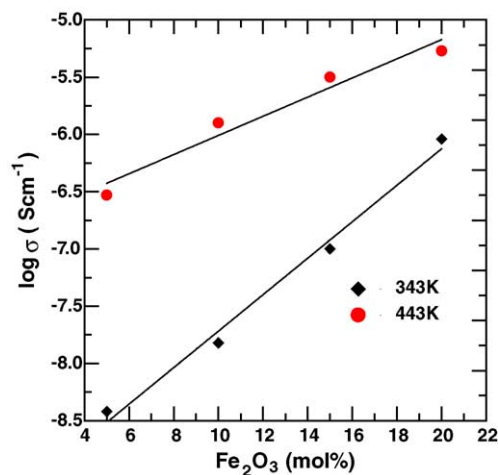


Fig. 4. Effect of  $\text{Fe}_2\text{O}_3$  content on dc conductivity,  $\sigma$ , at  $T = 343$  and  $443$  K for different glass compositions.

Table 1  
Data of  $T_g$  for various compositions

Glass no.	Nominal composition (mol%)			$T_g$ (K) at various heating rates $\alpha$ (K/min)					$B$ in $T_g = A + B \ln \alpha$	
	$Fe_2O_3$	$Bi_2O_3$	$Na_2B_4O_7$	10	15	20	25	30		35
1	5	20	75	677.2	680.2	683.2	685.5	687.9	689.8	10.04
2	10	15	75	678.6	681.9	684.2	686.8	689.8	691.2	10.01
3	15	10	75	680.5	684.0	687.0	689.1	692.0	693.5	10.45
4	20	5	75	682.7	686.5	688.5	691.8	694.1	695.7	10.37

endothermic peak corresponding to the glass transition, at a temperature  $T_g$ . Secondly, the crystallization processes show two exothermic crystallization peaks ( $T_{p1}$  and  $T_{p2}$ ), as confirmed above by XRD.

### 3.3.1. Glass transition

The variation of  $T_g$  with  $Fe_2O_3$  content for these glasses (Table 1) is shown in Fig. 6. There is a small increase in  $T_g$  by about 5.5 K as the  $Fe_2O_3$  content increased from 5 to

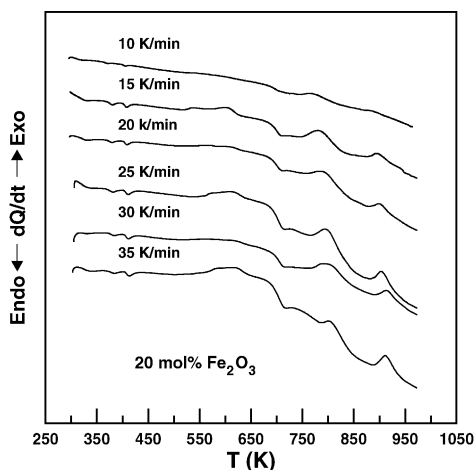


Fig. 5. Continuous heating DSC curves of  $20Fe_2O_3-5Bi_2O_3-75Na_2B_4O_7$  glass at different heating rates.

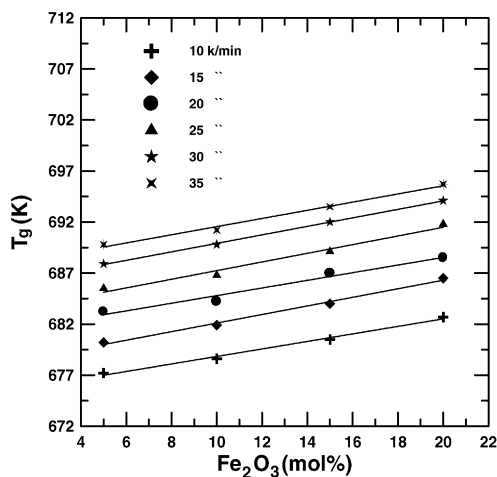


Fig. 6. Variation of  $T_g$  with composition for  $xFe_2O_3-(25-x)Bi_2O_3-75Na_2B_4O_7$  glasses with  $x = 5, 10, 15$  and  $20$  mol% at different heating rates.

20 mol%. The value of  $T_g$  varies by about 13 K (Table 1) as the heating rate is varied from 10 to 35 K/min. When  $Bi_2O_3$  is substituted for  $Fe_2O_3$ , the Fe–O–Fe bonds are broken and new bonds such as Fe–O–Bi and Bi–O–Bi bonds are probably formed, causing a decrease in conductivity and thermal stability with increasing  $Bi_2O_3$  content in the glasses [28].  $T_g$  represents the strength or the rigidity of the glass structure. Therefore, drastic changes in  $T_g$  cannot be expected by increase in  $Fe_2O_3$  content, which results in isostructural units of nearly same bond strength.

Two approaches are used to discuss the dependence of  $T_g$  on the heating rate  $\alpha$ . One is the empirical relationship of the form [29]

$$T_g = A + B \ln \alpha \quad (2)$$

where  $A$  and  $B$  are constants for a given glass composition. The results of Fig. 7 indicate the validity of this relationship for the  $xFe_2O_3-(25-x)Bi_2O_3-75Na_2B_4O_7$  (where  $x = 5, 10, 15$  and  $20$  mol%) glasses for all the heating rates range 10–35 K/min. The constant  $B$  in the above expression has a value of 10.21 for all the present glasses (Table 1).

The other approach is the use of the so-called Kissinger's formula [30] for the evaluation of the activation energy for glass transition,  $E_t$ . For homogeneous crystallization with spherical nuclei, it has been shown [31,32] that the

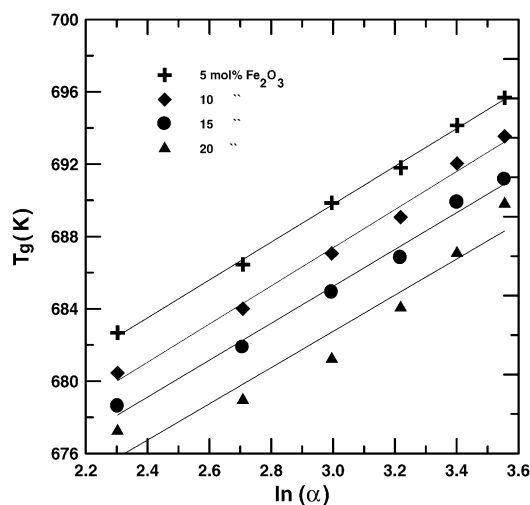


Fig. 7.  $T_g$  vs.  $\ln \alpha$  for different glass compositions.

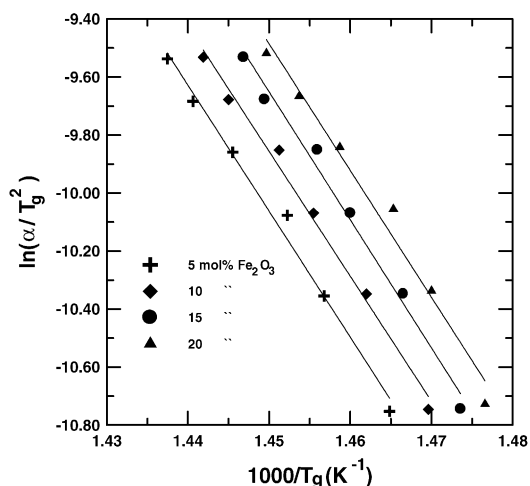


Fig. 8.  $\ln(\alpha/T_g^2)$  vs.  $1/T_g$  for different glass compositions.

dependence of  $T_g$  on  $\alpha$  is given by:

$$\ln\left(\frac{\alpha}{T_g^2}\right) = \frac{-E_t}{RT_g} + \text{const} \quad (3)$$

where  $R$  is the universal gas constant. Plots of  $\ln(\alpha/T_g^2)$  versus  $1000/T_g$  for these glasses indicated linearity for all the heating rates range 10–35 K/min (see Fig. 8).  $E_t$  is found to have a value of 3.97 eV.

### 3.3.2. Activation energy of crystallization

The values of  $T_p$  for two phases of the various compositions are listed in Table 2 for the six heating rates studied. Fig. 9(a) and (b) show, respectively the composition dependence of  $T_p$  for the two phases (Fig. 9) of the investigated glasses at various heating rates. For the first phase, the value of  $T_p$  shows nonlinear (Fig. 9(a)) small decrease as the  $\text{Fe}_2\text{O}_3$  content is increased from 5 to 20 mol% while for the second phase (Fig. 9(b)) the dependence of  $T_p$  on the  $\text{Fe}_2\text{O}_3$  content is linear.

For the evaluation of the activation energy for crystallization ( $E_c$ ) from the variation of  $T_p$  with  $\alpha$ , the Kissinger's

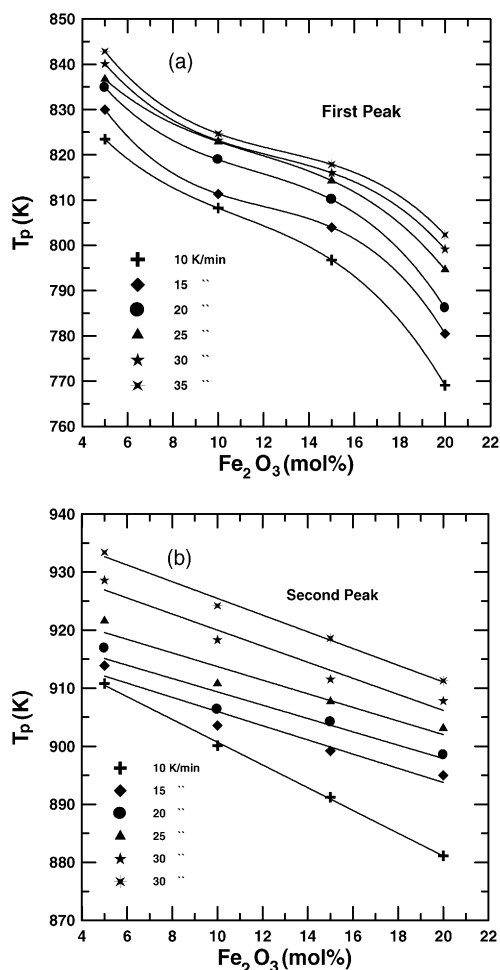


Fig. 9. Variation of  $T_p$  with composition for  $x\text{Fe}_2\text{O}_3-(25-x)\text{Bi}_2\text{O}_3-75\text{Na}_2\text{B}_4\text{O}_7$  glasses with  $x=5, 10, 15$  and  $20$  mol% at different heating rates for (a) the first peak and (b) the second peak, respectively.

equation can be used as follows:

$$\ln\left(\frac{\alpha}{T_p^2}\right) = \frac{-E_c}{RT_p} + \text{const} \quad (4)$$

Fig. 10 shows the  $\ln(\alpha/T_p^2)$  versus  $1000/T_p$  data for one of the compositions. Values of  $E_c$  for the two phases obtained from similar plots for the investigated glasses are listed in Table 3

The activation energies to be considered in a crystallization process are the activation energy for nucleation ( $E_N$ ),

Table 2  
Data of  $T_p$  and  $E_t$  for various compositions

Glass no.	$E_t$ (eV)	$T_p$ (K) at various heating rates $\alpha$ (K/min)						
		10	15	20	25	30	35	
1	3.76	823.4	830.0	834.8	836.7	840.1	842.8	$T_{p1}$
		910.8	913.9	916.6	921.6	928.6	933.4	$T_{p2}$
2	3.81	808.2	811.4	818.9	822.4	823.1	824.6	$T_{p1}$
		900.1	903.6	906.4	910.8	918.3	924.2	$T_{p2}$
3	3.71	796.7	803.9	810.1	814.3	816.0	817.8	$T_{p1}$
		891.2	899.2	904.2	907.7	911.5	918.6	$T_{p2}$
4	3.74	769.1	780.5	786.2	794.6	799.1	802.3	$T_{p1}$
		881.1	895.0	898.5	903.1	908.8	911.28	$T_{p2}$

Table 3  
Data of  $E_c$  for various compositions

Glass no.	$E_c$ (eV)	
	1st phase	2nd phase
1	3.71	3.90
2	3.45	3.58
3	3.07	3.23
4	1.83	2.49

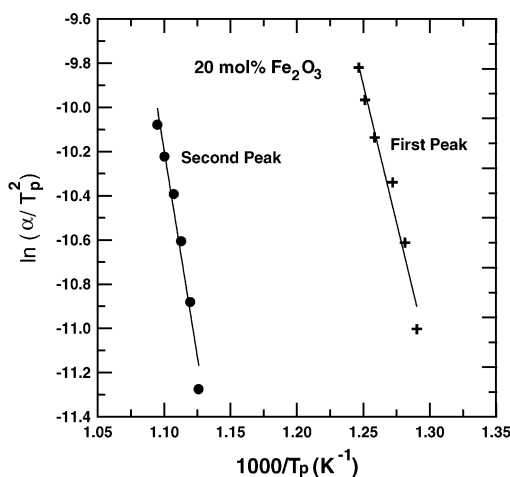


Fig. 10. Kissinger's plot of  $\ln(\alpha/T_p^2)$  vs.  $1/T_p$  for  $20\text{Fe}_2\text{O}_3\text{--}5\text{Bi}_2\text{O}_3\text{--}75\text{Na}_2\text{B}_4\text{O}_7$  glass for first and second peaks.

activation energy for crystal growth ( $E_G$ ) and that for the whole process of crystallization, called the activation energy for crystallization denoted by  $E_c$  [33]. The thermal analysis methods enable the determination of  $E_c$  [34,35]. It has been pointed out [36] that in non-isothermal measurements, generally due to a rapid temperature rise and big differences in the latent heats of nucleation and growth, the crystallization exotherm characterises the growth of the crystalline phase from the amorphous matrix; nucleation is more or less calorimetrically unobservable at temperatures below the crystallization exotherm, or it takes place very rapidly and immediately after overheating of the material in the initial stages of the crystallization exotherm, which results in the deformed beginning of the measured exotherm. Therefore, the analysis gives the value of the activation energy for crystal growth,  $E_G$ . Based on this, the value of  $E_c$  (listed in Table 3) can be taken to represent the activation energy for growth,  $E_G$ , of these glasses.

#### 4. Conclusions

Semiconducting  $x\text{Fe}_2\text{O}_3\text{--}(25-x)\text{Bi}_2\text{O}_3\text{--}75\text{Na}_2\text{B}_4\text{O}_7$  glasses with  $x=5, 10, 15$  and 20 mol% were prepared by the press-quenching technique from the melts and the dc conductivity was discussed in terms of SPH model. The inverse temperature dependence of  $\log(\sigma)$  in the range 300–473 K gave linearity but deviated from linearity for temperatures less than  $\theta_D/2$ . In the low temperature region ( $T < \theta_D/2$ ), the transport is attributed to be electronic, while at high temperature region ( $T > \theta_D/2$ ) the  $\text{Bi}^{3+}$  and  $\text{Na}^+$  ions may become mobile and participate in the conduction

process. The crystallization exotherms of these glasses have been analyzed under non-isothermal conditions. Using the Kissinger method, different activation energies are obtained and the composition dependence of  $E_c$  is also discussed. It is assumed that the Kissinger activation energy comes mainly from the growth activation energy.

#### References

- [1] M.M. El-Desoky, Phys. Stat. Sol. (a) 195 (2003) 422.
- [2] M.M. El-Desoky, M.Y. Hassaan, Phys. Chem. Glasses 43 (2002) 1.
- [3] T. Hirashima, F. Tanaka, Seramikkusu Ronbunshi 97 (1989) 1150.
- [4] K. Tanaka, T. Yoko, N. Nakano, M. Nakamura, K. Kamiya, J. Non-Cryst. Solids 125 (1990) 264.
- [5] S. Nakamura, N. Ichinose, Jpn. J. Appl. Phys. 28 (1989) 984.
- [6] S. Nakamura, N. Ichinose, J. Non-Cryst. Solids 95–96 (1987) 849.
- [7] A.C. Wright, S.A. Feller, A.C. Hannon (Eds.), in: Borate Glasses, Crystals and Melts, Society of Glass Technology, Sheffield, 1997.
- [8] Y.B. Dimitriev, A.C. Wright (Eds.), in: Borate Glasses, Crystals and Melts: Structure and Applications, Society of Glass Technology, Sheffield, 2000.
- [9] P. Becker, Cryst. Res. Technol. 38 (2003) 74.
- [10] N.F. Mott, J. Non-Cryst. Solids 1 (1968) 1.
- [11] I.G. Austin, N.F. Mott, Adv. Phys. 18 (1969) 41.
- [12] M.M. El-Desoky, J. Mater. Sci. Mater. Electron. 14 (2003) 215.
- [13] M.M. El-Desoky, I. Kashif, Phys. Stat. Sol. (a) 194 (1) (2002) 89.
- [14] B. Roling, K. Funke, J. Non-Cryst. Solids 212 (1997) 1.
- [15] T. Holstein, Ann. Phys. 8 (1959) 343.
- [16] C.A. Agnelli, W. Sichina, Ann. N.Y. Acad. Sci. 279 (1976) 53.
- [17] M.H. Cohen, G.S. Grest, Phys. Rev. B 21 (1980) 4113.
- [18] J. Jäckle, Rep. Prog. Phys. 49 (1986) 171.
- [19] P. Tuinstra, P.A. Duine, J. Sietsma, A. van den Beukel, Acta Metall. Mater. 7 (1995) 2815.
- [20] H.E. Kissinger, Anal. Chem. 29 (1957) 32.
- [21] D.W. Henderson, J. Non-Cryst. Solids 30 (1979) 301.
- [22] G. Ruitenbergh, E. Woldt, A.K. Petford-Long, Thermochim. Acta 378 (2001) 97.
- [23] H. Doweidar, A.A. Megahed, I.A. Gohar, J. Phys. D: Appl. Phys. 19 (1986) 1939.
- [24] H.H. Qiu, H. Sakata, T. Hirayama, J. Chin. Ceram. Soc. 24 (1996) 58.
- [25] M.M. El-Desoky, K. Tahoon, M.Y. Hassaan, Mater. Chem. Phys. 69 (2001) 180.
- [26] M.M. El-Desoky, M.Y. Hassaan, M.H. El-Kottamy, J. Mater. Sci. Mater. Electron. 9 (1999) 447.
- [27] D. Deal, M. Burd, R. Brunstein, J. Non-Cryst. Solids 54 (1993) 207.
- [28] H.H. Qiu, T. Ito, H. Sakata, Mater. Chem. Phys. 58 (1999) 243.
- [29] M. Lasocka, Mater. Sci. Eng. 23 (1976) 173.
- [30] H.E. Kissinger, J. Res. Nat. Bur. Stand. 57 (1956) 217.
- [31] H.S. Chen, J. Non-Cryst. Solids 27 (1978) 257.
- [32] J.E. Shelby, J. Non-Cryst. Solids 34 (1979) 111.
- [33] S. Mahadevan, G. Giridhar, A.K. Singh, J. Non-Cryst. Solids 88 (1986) 11.
- [34] S. Ranganathan, M. Von Heimendahl, J. Mater. Sci. 16 (1981) 2401.
- [35] M. Von Heimendahl, G. Kuglstatler, J. Mater. Sci. 16 (1981) 2405.
- [36] E. Illekoova, J. Non-Cryst. Solids 68 (1984) 153.